The 8th International Conference on
Structural Health Monitoring of Intelligent Infrastructure
Brisbane, Australia | 5-8 December 2017

Visualization of Strain and New Strain Measurement Technique

M. Omachi [1], S. Umemoto [1], T. Takaki [2], K. Matsuo [1],
N. Miyamoto [1], I. Ishii [2], T. Aoyama [2]
[1] *Keisoku Research Consultant Co., Japan, Email:* umemoto@krcnet.co.jp
[2] *Hiroshima University, Japan*

Abstract

A strain visualization device and a new strain measurement technique were developed in response to the need for health monitoring of rapidly-aging structures. The device, which is called the "Strain Visualization Sheet," utilizes the principle of Moiré fringes. As a result of repeated improvements to enable application to field measurements, a self-temperature compensated strain visualization sensor was realized. A revolutionary strain measurement technique was also established, which not only enables quantitative visualization of strain, but also simple measurement with an ordinary digital camera by personnel without special skills. Strain visualization resolution of 50μm/m and measurement error of <20μm/m were confirmed in a verification of accuracy in the laboratory with a calibration device. In a comparison with a conventional strain gauge in a tensile test of steel specimens, the same <20μm/m level of error in the strain value was also obtained by this measurement technique, verifying the appropriateness of the measurement technique and the Strain Visualization Sheet as a sensor. Based on these results, Strain Visualization Sheets were applied in two fields. As a result, stable strain data were obtained and applicability to field measurement was verified. With the application of the Strain Visualization Sheet to structural health monitoring, acquisition of strain information on structures are economical and simple. As a result, more advanced regular visual inspections are possible, and strain information on structures can be obtained at low cost.

1. Introduction

Health monitoring of structures is expected to have a variety of benefits, including a higher level of inspection, labor-saving in inspections and early discovery of abnormalities, and also assist in early recovery in disasters and other abnormal cases. In recent years, however, health monitoring been limited to only some structures due to problems such as the condition of public finances, and is also not performed adequately, even in visual inspections. The largest reason for the failure to implement health monitoring of structures is the problem of cost. In addition to the cost of installation, maintenance costs also increase as more sophisticated sensors are used. Moreover, if frequent maintenance of the monitoring equipment itself is necessary, equipment maintenance costs will also increase, and depending on the scale of the structure, this may result in reversing the logical order of things. Therefore, focusing on strain, which is one monitoring item, we developed a device called the Strain Visualization Sheet with the aim of establishing a remote, noncontact strain measurement technique that enables simple measurement by personnel without special skills (Omachi, M. et al. 2015). The Strain Visualization Sheet is a new sensor for use in strain measurements utilizing the principle of Moiré fringes, and has the following distinctive features.

(1) Quantitative visualization of strain is possible.

(2) Because the Strain Visualization Sheet uses absolutely no electrical elements, a power source is not necessary and device life is not determined by electrical failure.

(3) For the same reason, the Strain Visualization Sheet is not affected by electrical noise.

(4) Strain can be measured by a remote, noncontact method with higher accuracy than is possible by visual inspection by using a general digital camera, etc.

(5) Maintenance is easy.

Recently, we developed a self-temperature compensated type of Strain Visualization Sheet for application to field measurements, and after repeated improvement to solve several problems in field measurement, we succeeded in practical application of the new device. This paper presents an outline of the Strain Visualization Sheet, which is a new strain measurement technology. The results of a performance verification are reported, and examples of application of Strain Visualization Sheet in the field are also introduced.

2. Measurement Principle of Strain Visualization Sheet

As shown in Fig. 1(1), when line grating 1 with pitch p and line grating 2 with a pitch $p+\Delta p$ which is Δp ($<<p$) larger than the pitch of line grating 1 are superimposed, a striped pattern with a pitch W larger than that of line gratings 1 and 2 appears. This pattern is called a Moiré fringe. The Strain Visualization Sheet utilizes the principle of the Moiré fringe. The relationship between the pitch of the line gratings and the pitch of the Moiré fringe can be expressed by Eq. (1), and pitch p can be displayed visually enlarged by $(p+\Delta p) / \Delta p$ by the Moiré fringe. This magnification factor is M.

$$W = \frac{p + \Delta p}{\Delta p} \cdot p \tag{1}$$

In order to enhance visibility (legibility), a Moiré fringe with a high magnification ratio is obtained by treating a number n of stripes with pitch p on line grating 2 as one unit, and arranging this at intervals of $np+\Delta p$. The pitch of the Moiré fringe which is formed under this condition can be expressed by Eq. (2), and the magnification factor is $(np+\Delta p) / \Delta p$.

$$W = \frac{np + \Delta p}{\Delta p} \cdot p \tag{2}$$

The amount of shift Δx_m of the Moiré fringe in direction (A) when line grating 1 moves Δx in direction (A), as shown in Fig. 1(2), is expressed by Eq. (3). This means that displacement Δx can be displayed visually enlarged by M times. It is possible to measure the strain level by this principle.

$$\Delta x_m = M \cdot \Delta x \tag{3}$$

In the same manner, if a grating in character form (character grating) is used in place of line grating 1, as shown in Fig. 2, the amount of shift when the character grating is moved in direction (A) can be displayed by changes in the characters, as in (i') to (iii'). In visualization of strain, numbers corresponding to the amount of generated strain are displayed by arranging the character grating in the form of a strain scale and adjusting the magnification factor.

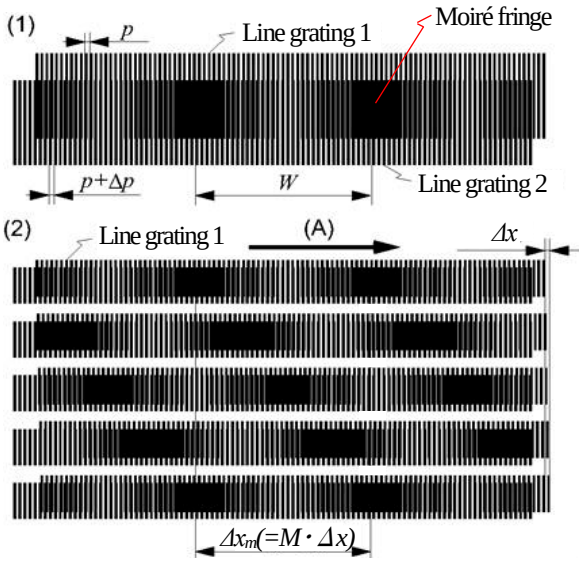

Fig. 1 Example of a moiré fringe

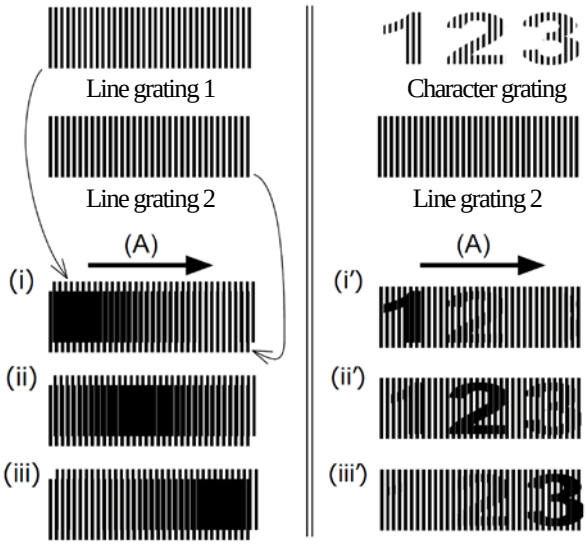

Fig. 2 A moiré fringe with characters

3. Strain Visualization Sheet

3.1 Structure of Strain Visualization Sheet

The structure and appearance of the Strain Visualization Sheet are shown in Fig. 3 and Fig. 4, respectively. The device comprises the two glass plates that form the Moiré fringe pattern and a steel temperature compensation plate for temperature compensation, and is assembled into a unit by using two fixing rings. The length, width and thickness of the Strain Visualization Sheet are 120 mm, 14 mm and 8 mm, respectively, and the gauge length is 105 mm. The Strain Visualization Sheet consists of three fringe types. The Moiré fringes in the top and middle line change according to the strain. The top line shows character patterns in the form of a scale with an interval of 100 μm/m, and allows the user to read strain values directly with the unassisted eye. The middle line is a simple Moiré fringe for strain measurement by image processing, and the bottom line is a reference Moiré fringe for improvement of image cropping accuracy in image processing.

3.2 Specification of Grating Pattern

The pitch p, Δp and number of repetitions n of the grating pattern in the visualization part on the top line are 0.1 mm, 0.01 mm and 73, respectively, and the magnification factor M = 730x. In the image processing part on the middle line, the pitch and number of repetitions of the grating pattern p, Δp and n are 0.07 mm, 0.00025 mm and 1, and M = 280x. Because grating pattern generation technology has improved dramatically, it has become possible to set the pitch p and Δp on the image processing part on the middle line to smaller values than were used until now, and it is also possible to secure the same magnification factor M as in the past, even with the number of repetitions n = 1.

3.3 Structure of Pattern Glass

Fig. 5 shows the structure of the pattern glass. Photomask technology is used in generating the pattern on the glass. Grating pattern 1 is generated on the back side of the front glass. The back glass is first coated with a white undercoat, and grating pattern 2 is then generated. After the patterns are generated a clear overcoat is applied to both line gratings.

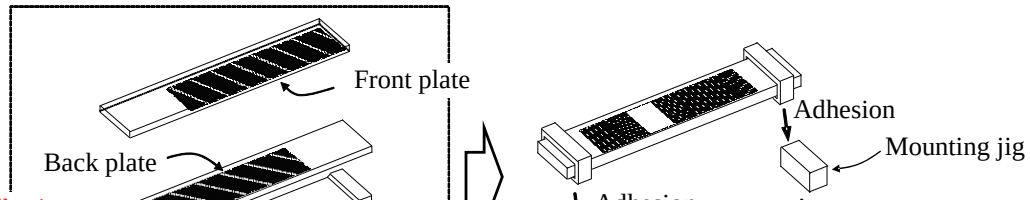

Fig. 3 Structure of Strain Visualization Sheet

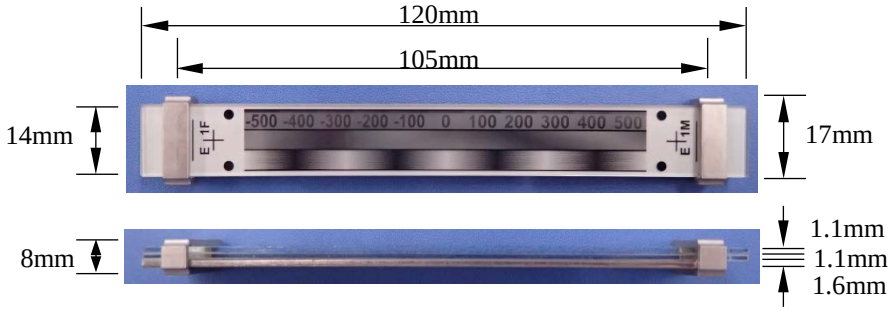

Fig. 4 Appearance of Strain Visualization Sheet

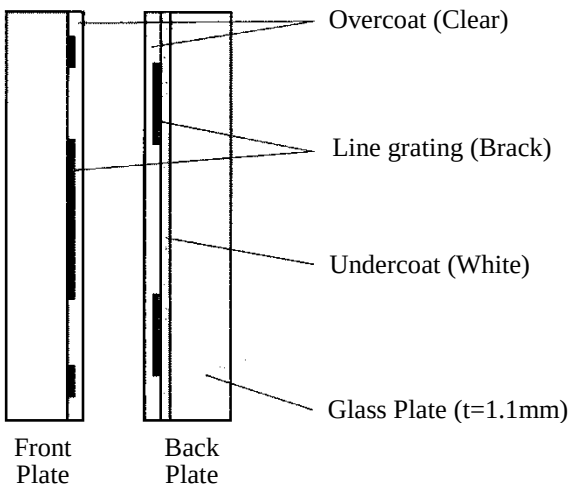

Fig. 5 Structure of Pattern glass

4. Verification of Accuracy

4.1 Test Device

The appearance of the test device and the displacement control unit are shown in Fig. 6 and Fig. 7, respectively. The test device consists of the displacement stage, laser displacement meter (repeatability: 0.05 μm) and their control PC, a USB camera (resolution: 2 x 10^6 pixels) for use in photographing the Strain Visualization Sheet and a real-time image processing device. The USB camera was set at a height of 90 cm above the Strain Visualization Sheet, and lighting was provided to maintain a constant intensity of illumination.

4.2 Test Method

After the initial value was measured, displacement (strain ε = 45 μm/m equivalent) was applied with a pitch of 5 μm to the Strain Visualization Sheet by the test device, and the Strain Visualization Sheet was photographed continuously with the USB camera. Strain was calculated from the continuous photographed images in real time by the real-time image processing device, and the strain values were recorded at intervals of 5 μm.

4.3 Visual Measurement

Fig. 8 shows the change of the strain values in the visualization part. The strain values were obtained by reading the central value in the numbers that could be recognized visually to a half between indicated numbers. From the verification results, it can be understood that the strain values can be visualized with accuracy of ±50 μm/m for the strain generated at each 90 μm/m.

4.4 Measurement by Image Processing

Fig. 9 shows the results of measurements of the strain generated by the displacement stage obtained by image processing of the Strain Visualization Sheet. The results of measurements by image processing showed extremely good agreement with the actual generated strain. Error was –8 μm/m to +15 μm/m, confirming that strain can be measured with higher accuracy than by measurement by visual inspection.

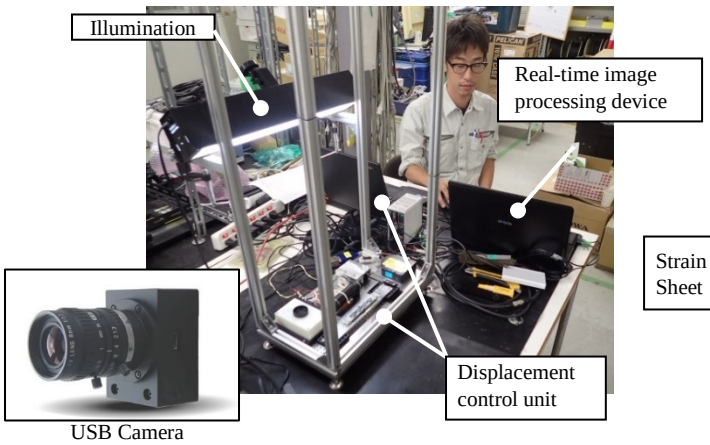

Fig. 6 Appearance of test setup

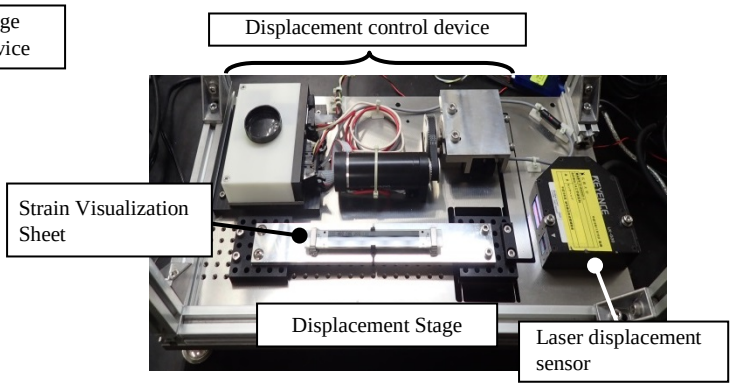

Fig. 7 Displacement control unit

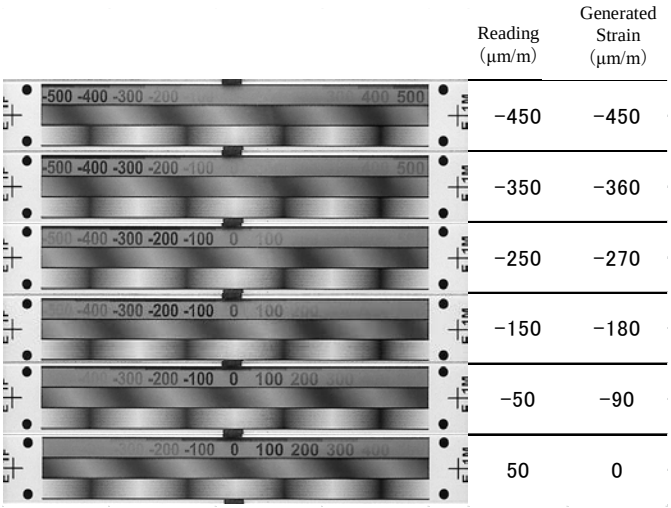

Fig. 8 Change in strain value of visualization part

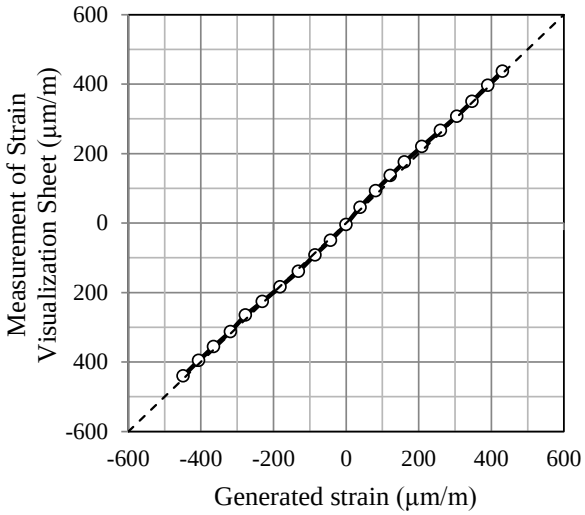

Fig. 9 Image processing result

5. Comparative Verification by Tensile Test

5.1 Test Piece

Fig. 10 shows the tensile test piece (JIS Z2201, No. 14). A Strain Visualization Sheet and a strain gauge as an object of comparison were arranged adjacent to each other on both sides of the test piece at the test piece center. The gauge length of the strain gauge was 90 mm.

5.2 Test Method

The test piece was set in the test machine (rated capacity: 1 000 KN) as shown in Fig. 11, and loading was applied in steps of 20 kN at a constant rate so as not to apply impact to the test piece. Loading was continued to a maximum of 140 kN, after which the load was removed in the same manner. The Strain Visualization Sheets on both side of the test piece were photographed with a general digital camera (Fig. 12) while keeping the load at each 20 kN step. The values of the strain gauges were also recorded at the same time.

The strain calculation application shown in Fig. 13 was used in calculations of the strain values. This application, which was developed for use in field measurements, calculates strain from the static images photographed by the digital camera. Strain is calculated by the procedure of (1) reading the static image, (2) extracting the image of the Moiré fringe, (3) fitting the measured value and the theoretical value of the luminance distribution (sine approximately curve) of the Moiré fringe and (4) calculating the strain value from the phase difference with the original image. In actual operation, the operator simply selects the black circles at the four corners of the Strain Visualization Sheet in order and clicks the analysis button.

5.3 Verification Results

Fig. 14 shows the relationship of load and strain during the loading cycle, and Fig. 15 shows the results during the unloading cycle. The average values of the strain on the two sides of the test piece are shown for both the strain gauges and the Strain Visualization Sheets.

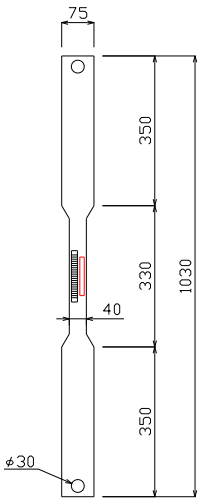

: Strain gauge

unit : mm : Strain Visualization Sheet

Fig. 10 Test Piece for Tensile Test

Fig. 11 Testing scene

OLYMPUS STYLUS TG-3 Tough

Fig. 12 Digital camera

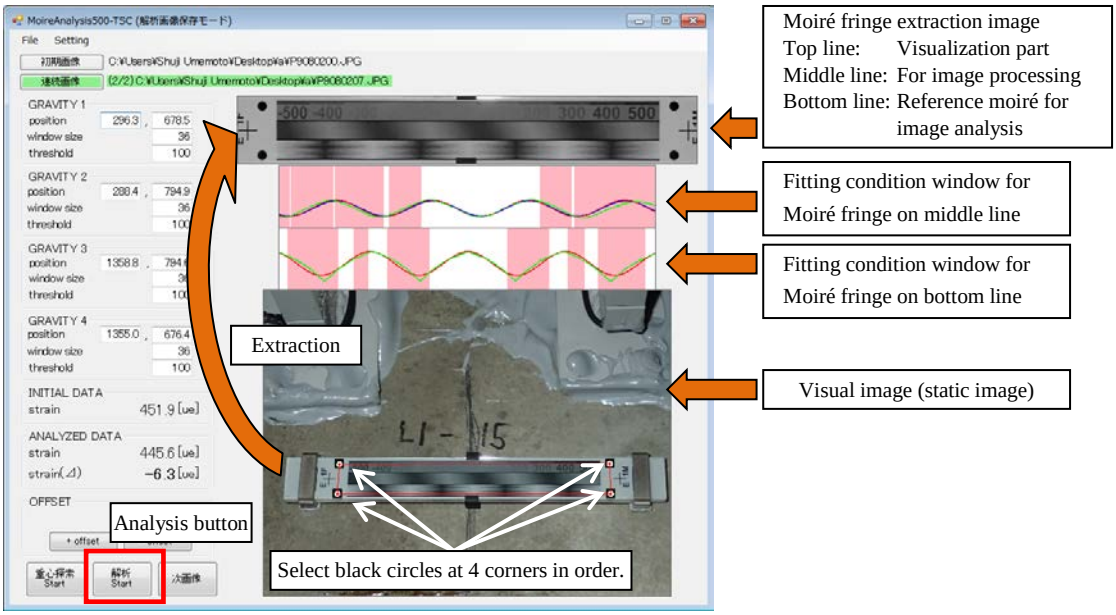

Fig. 13 Strain calculation application

During loading, the values of the Strain Visualization Sheet showed extremely good agreement with the values of the stain gauge, the maximum difference being 14 μm/m. Although the difference with the strain gauge during unloading was somewhat larger than during loading, the average difference was 20 μm/m and the maximum difference was 32 μm/m. Thus, this verification, which assumed field measurement, verified the fact that strain can generally be measured with high accuracy by the Strain Visualization Sheet.

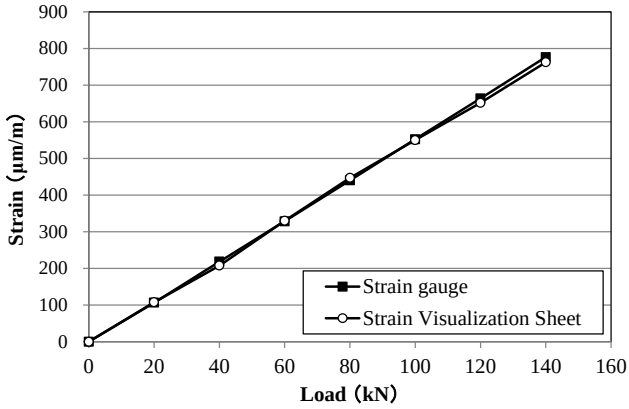

Fig. 14 Relationship of load and strain (loading)

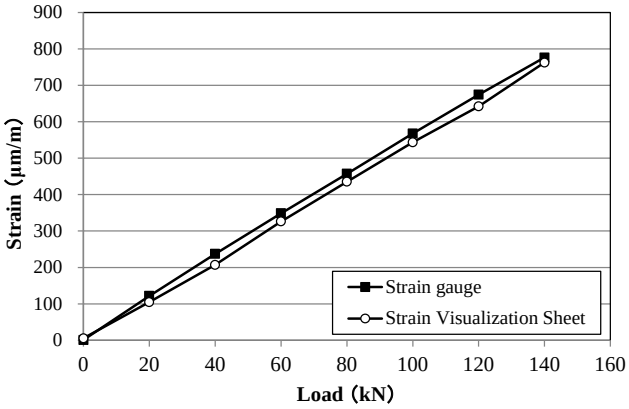

Fig. 15 Relationship of load and strain (unloading)

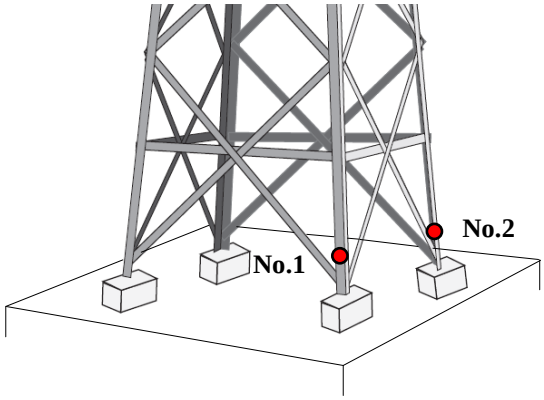

Fig. 16 Measurement positions

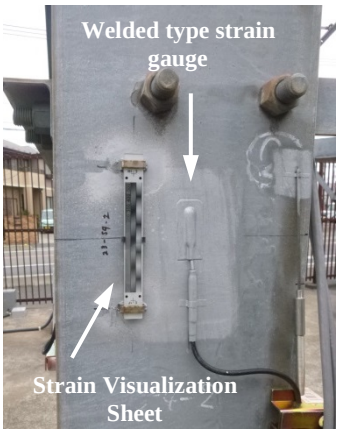

Fig. 17 Condition of measurement device installation

6. Application to Field Measurement

In order to verify the applicability of the Strain Visualization Sheet to field measurement, Strain Visualization Sheets were applied to a steel power transmission tower in Saitama Prefecture, Japan and to a telecommunications tunnel in Tokyo, and strain measurements were performed.

6.1 Strain Measurement of Steel Power Transmission Tower

6.1.1 Outline of Measurement

As shown in Fig. 16, Strain Visualization Sheets were applied to two positions on the legs of the steel transmission tower. In addition to installing these Strain Visualization Sheets on the tower legs, welded type strain gauges (gauge length: 5 mm) were also installed adjacent to the Strain Visualization Sheets for comparison. The condition of installation is shown in Fig. 17.

6.1.2 Measurement Results

The strain measurement results are shown in Fig. 18 (position No. 1) and Fig. 19 (position No. 2). As the measured strain data for the Strain Visualization Sheet, static images were photographed by using digital cameras, and strain was calculated by the strain calculation application software.

Although the amount of change in the strain is slight and the number of measurements is small, the measured values obtained by the Strain Visualization Sheet at the present point in time are trending at a difference of 10-50 μm/m in comparison with the measured values by the welded type strain gauge, and stable measured data are being obtained.

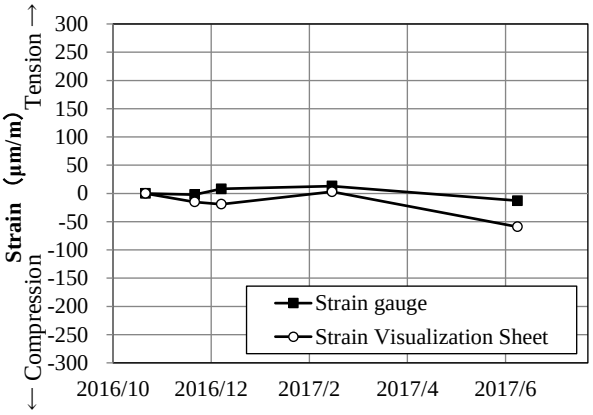

Fig. 18 Strain measurement results (position No. 1)

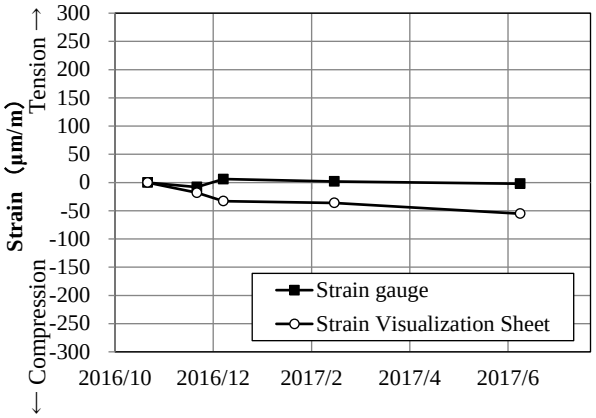

Fig. 19 Strain measurement results (position No. 2)

6.2 Strain Measurement of Telecommunications Tunnel

6.2.1 Outline of Measurement

In this test, the object of measurement was the lining concrete of a telecommunications tunnel. As the measurement locations, two locations with different environmental conditions ((1) Dry condition, (2) Wet condition) were selected.

A Strain Visualization Sheet was installed on the lining concrete, and a strain transducer (gauge length: 100 mm) and a metal base strain gauge were installed near the Strain Visualization Sheet as objects of comparison. The stainless steel type metal base strain gauge was used in order to prevent insulation degradation due to moisture from the concrete. A thermocouple type thermometer was also installed to measure the ambient temperature. Fig. 20 shows the condition of installation of these measuring devices.

6.2.2 Measurement Results

Fig. 21 shows the strain measurement results. The strain data measured by the Strain Visualization Sheet were obtained by photographing static images with a digital camera and calculating the strain values with the strain calculation application software.

At the measurement point under the dry environment, the strain values were approximately in agreement from the start of measurement until about 4 months. However, after 4 months, a maximum difference of approximately 200 μm/m was observed in comparison with the conventional measurement method using the strain gauge and the strain transducer. Since we cannot rule out the possibility that a malfunction occurred in the strain transducer, strain gauge or Strain Visualization Sheet after the measurements in February 2017, we plan to continue checking the trend of the measured data and investigate whether a sensor malfunction of other problem occurred.

At the measurement point under the wet environment, no changes in the strain data were observed after the measurement in February 2017. Although a difference of approximately 100 μm/m occurred between the Strain Visualization Sheet and the strain gauge/strain transducer, the cause is not known at the present time. The strain gauge at the measurement point under the wet environment failed about 1 month after the start of measurements.

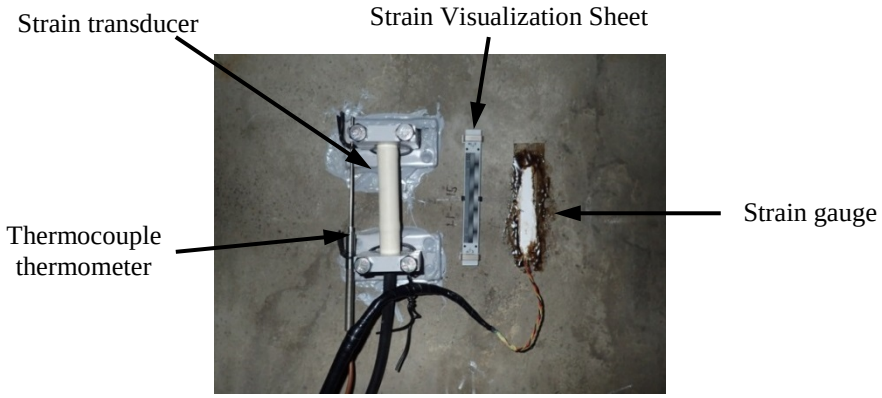

Fig. 20 Condition of installation of measuring devices

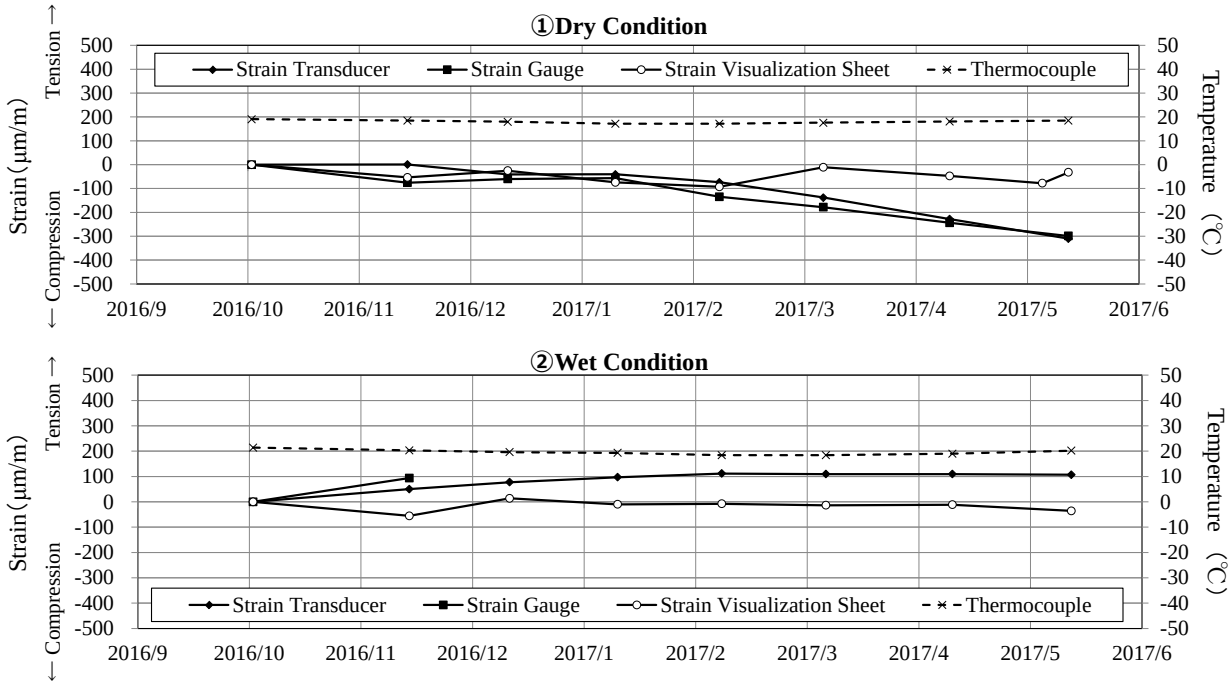

Fig. 21 Strain measurement result

7. Conclusion

To respond to the need for health monitoring of structures, the authors developed and successfully realized practical application of a device called the Strain Visualization Sheet as a new strain measurement technology which enables quantitative visualization of strain. In a verification of measurement accuracy in laboratory tests, highly accurate measurements were possible in both measurement by visual inspection and measurement by image processing. The possibility of measurements at a level that enables practical application was also demonstrated in a tensile test of steel material assuming field measurement. Although there are a few examples of application to actual field measurement, this research showed the possibility of practical application in long-term measurement. In the future, the authors plan to accumulate actual results of practical application in the field and improve the completeness of the Strain Visualization Sheet.

References

Omachi, M. et al., 2015, 'Verification of Strain Visualization Sheet with Aim of Field Application', *Proceeding of the 7th International Conference on Structural Health Monitoring of Intelligent Infrastructure (SHMII-7)*, Torino,Italy, 1-3 July.